Asian Journal of Chemistry; Vol. 28, No. 4 (2016), 853-858

ASIAN JOURNAL OF CHEMISTRY

http://dx.doi.org/10.14233/ajchem.2016.19538

Molecular Recognition and Solubility of Mefenamic Acid in Water

S.K. ABDUL MUDALIP[1], M.R. ABU BAKAR[2], P. JAMAL[3], F. ADAM[1,*] and Z.M. ALAM[3]

[1]Faculty of Chemical & Natural Resources Engineering, University Malaysia Pahang, Gambang, 26300 Kuantan, Pahang, Malaysia
[2]Department of Pharmaceutical Technology, Kulliyyah of Pharmacy, International Islamic University Malaysia, Bandar Indera Mahkota, 25200 Kuantan, Pahang, Malaysia
[3]Department of Biotechnology Engineering, Kulliyyah of Engineering, International Islamic University Malaysia, 50728 Kuala Lumpur, Malaysia

*Corresponding author: Fax: +60 9 5492889; Tel: +60 9 5492824; E-mail: fatmawati@ump.edu.my

Received: 30 July 2015; *Accepted*: 28 September 2015; *Published online*: 30 December 2015; AJC-17704

Molecular dynamics simulations were performed using COMPASS force field and Ewald summation method that are available in the Material Studio simulation package. The aim of this work is to investigate the solubility and intermolecular interactions (*i.e.*, hydrogen bonding) of water with mefenamic acid. The solubility of mefenamic acid in water is lower than the ideal solubility. The results of the simulation show that the density, diffusion coefficient and radial distribution functions calculated for water are comparable with the literature. Analysis of radial distribution functions in the binary system of mefenamic acid/water shows low hydrogen bond formation between mefenamic acid and water molecules as well as diffusivity. In addition, the strength of the interaction is much lower than that of hydrogen bonds formed between molecules of water. These findings suggest low diffusivity and poor solubility characteristic of mefenamic acid in water.

Keywords: Solubility, Molecular dynamics simulation, Hydrogen bonding, Diffusivity.

INTRODUCTION

Mefenamic acid [(2-(2,3-dimethylphenyl)aminobenzoic acid] is a commonly used non-steroidal anti-inflammatory drug (NSAID) for the treatment of postoperative and traumatic inflammation as well as an analgesic treatment of rheumatoid arthritis and an antipyretic for acute respiratory tract infection [1-3]. This drug is also recommended for the management of pain caused by menstrual disorders [4,5]. Fig. 1 illustrates the chemical structure of the mefenamic acid molecule, which is comprised of amine, carboxylic, benzyl ring and methyl groups. As seen, a strong intramolecular interaction is formed between the carboxylic group and nitrogen atoms in the mefenamic acid molecule [3]. Pedersen [6] revealed that a characteristic of mefenamic acid that limits its bioavailability is its low solubility value in water. Based on the principle of 'like dissolves like', it is expected that the carboxylic and amino groups of the mefenamic acid molecule that are polar protic in nature will show good solubility in polar protic and dipolar aprotic solvents [7]. Although water is a polar protic solvent, no trace of mefenamic acid was found during a solubility study in water at room temperature [8]. The study reported that the mefenamic acid is non-soluble at 298 K, while, at 313 K, the solubility value is only 0.00001 mole fraction [8].

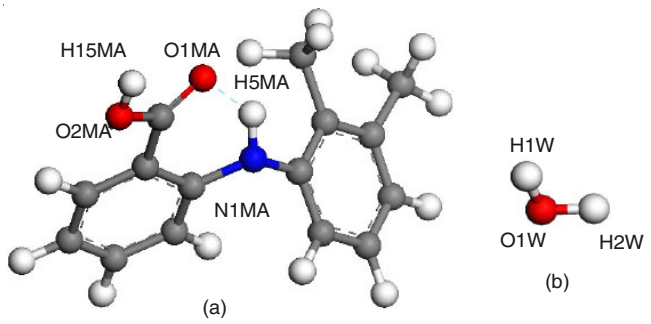

Fig. 1. (a) Chemical structure of a mefenamic acid molecule with partial labelling; (b) Water; Colour representation: white: hydrogen; grey: carbon; blue: nitrogen and red: oxygen

Understanding the solubility phenomenon of drug dissolution is a major interest in pharmaceutical research [9,10]. Experimental methods alone are insufficient to characterize the interactions involved at the molecular level that limit the solubility or dissolution of a pharmaceutical compound of interest in a particular solvent. Molecular dynamics (MD) simulation, on the other hand, can provide calculation and projection of motion for chemical species using Newton's laws [11-13]. Molecular dynamics simulation is ideally suited to explore several structures at the atomic level and also dynamic

processes that are impossible to investigate using experimental approaches. In recent years, significant progress has been made toward understanding polymorphism [14], crystal habits [15], solubility or dissolution processes [16] and glass transition phase behaviours [17] using molecular dynamics simulation.

In this work, molecular dynamics simulation was performed to fill the gap and provide molecular insight on mefenamic acid solubility in water. A third-generation force field, the condensed-phase optimized molecular potentials for atomistic simulation studies (COMPASS) force field developed by Sun [18] was used to model the system. To our best of knowledge, this is the first time molecular dynamics simulation was used to examine the intermolecular forces between mefenamic acid and water molecules. The diffusion coefficients and the radial distribution functions (RDFs) generated from the simulation trajectories were discussed.

EXPERIMENTAL

The molecular structures of the mefenamic acid and water molecules illustrated in Fig. 1 were sketched in Material Studio 5.5 (Accelrys, Inc., San Diego, USA). The geometry optimization and energy minimization of the molecules were performed using Smart minimizer. The cubical simulation box with the periodic boundary for the random configuration of pure water and the binary mixture of water and mefenamic acid were constructed using the amorphous cell package. The densities of water and mefenamic acid tabulated in Table-1 were obtained from the literature [19,20]. The simulations were performed at 298 K and 1 atm using the COMPASS force field and Ewald summation technique. Ewald summation was used to address the long-range electrostatic interactions [21]. Initially, a 250 ps calculation was performed in a constant number of moles, volume and energy (NVE) ensemble, where molecules are allowed to move freely. The simulation was then continued in the constant number of moles, pressure and temperature (NPT) ensemble for 2000 ps. Nose [22] and Berendsen *et al.* [23] assumption methods were used in the number of moles, pressure and temperature ensemble to maintain the system at the required temperature and pressure. A time step of 1.0 fs was used during the calculation. Various radial distribution functions between each pair of atoms defined in Fig. 2 were calculated at the end of the simulation. These radial distribution functions represent the distances between each pair of atoms which averaged and normalized to the radial distribution function of an ideal gas of the same density [24]. The following equation is used to describe radial distribution function:

$$g_{xy}(r) = \frac{\left\langle N_y(r, r+dr)\right\rangle}{\rho_y 4\pi r^2 dr} \quad (1)$$

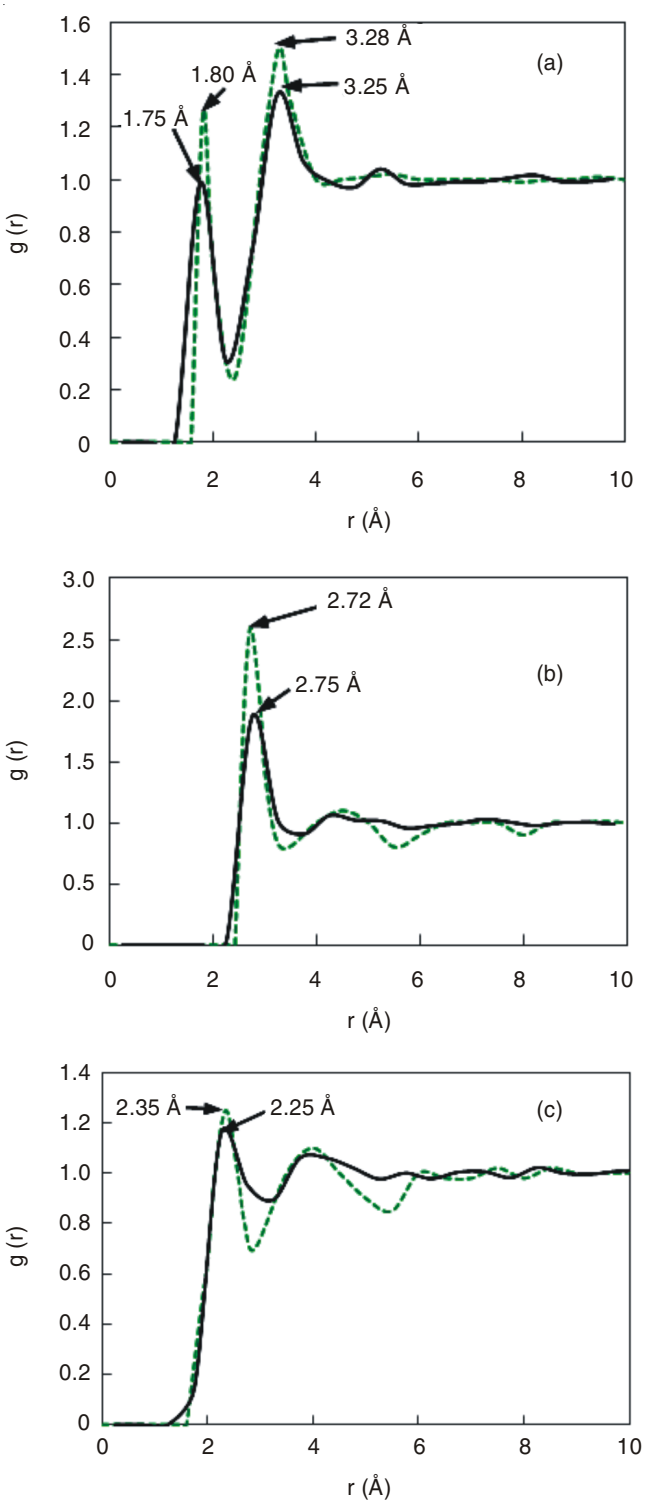

Fig. 2. g (r) plots for pure water showing molecular interactions between: (a) O1W···H1W; (b) O1W···O1W and (c) H1W···H1W. The solid line represents the RDF obtained in this work, while the green dashed line represents the RDF reported in the literature [Ref. 26]

TABLE-1
SIMULATION DATA

System	Number of molecules	Density (g/cm^3)	Equilibrated cell size: A × B × C [Å^3]
Water	250	0.997 [17]	19.57 × 19.57 × 19.57
Mefenamic acid/Water	25/250	1.136[a]	24.88 × 24.88 × 24.88

[a]This value was calculated using $\rho_{sol} = [(L + S)/(L/\rho_L + S/\rho_S)]$, where ρ_{sol} is the density of solution, L is the mass of solvent, S is the mass of solute, ρ_L is the density of the solvent and ρ_S is the density of the solute [Ref. 7]. The density of mefenamic acid used in this calculation was 1.268 g cm^{-3} [Ref. 20]

where r is a spherical radius distance from the reference atom, ρ_y is a density of a y atom, $<N_y(r,r + dr>$ is the number of y atoms in a shell of width Δr at distance r and x is the reference atom [25]. A self-diffusion coefficient D was estimated from the slope of the mean square displacement (MDS) plot *versus* time t using the Einstein equation [26]:

$$MSD = 6Dt + C \quad (2)$$

RESULTS AND DISCUSSION

Validation of simulation method: For validation of the simulation method, the radial distribution functions of pure water obtained in this work were compared with those of Mark and Nilson [26] who reported a simulation for water using an original SPC/E model at 298 K. In general, the radial distribution function patterns concur with the literature. Although the intensity of the radial distribution function peaks shown in Fig. 2 is quite low, the radii of the first peaks are almost the same as those of Mark and Nilson [26]. The first peaks observed for O1W···H1W, O1W···O1W and H1W···H1W are at 1.75, 2.75 and 2.25 Å, respectively. O1W···H1W shows the nearest neighbour interaction and thus represents the strength of hydrogen bonding present in the structure of pure water. The calculated deviation is less than 10 %. The slight differences in peak intensity and the radius of the first peak are probably due to differences in the force field type and the number of water molecules used during the simulation. Mark and Nilson [26] used 901 water molecules in their simulation while this work used only 250 water molecules.

Table-2 shows the deviation between simulated density and temperature of the water and a binary mixture of mefenamic acid/water when setting parameters at ambient conditions. As seen, the deviations are slightly small, which are less than 6 %. Sun [18] reported about a 6 % deviation in the density values during the simulation of 150 organic structures with the COMPASS force field. As the deviation obtained in this work is quite small, it can be suggested that the use of the COMPASS force field and the Ewald summation method can produce good simulation results.

Mean-squared displacement (MSD): Fig. 3 illustrates the MSD plots for pure water and a binary mixture of mefenamic acid/ water. The calculated diffusion coefficients for water in the pure system and the binary system are 5.642×10^{-9} and 3.193×10^{-9} m^2 s^{-1}, respectively. The calculated self-diffusion coefficient of pure water at 298 K is comparable with the literature value [26], which is 5.85×10^{-9} m^2 s^{-1}, a deviation of only 3.56 %. Comparisons for the diffusivities of water and mefenamic acid in the mefenamic acid/water system are unable to be made as they have yet to be reported in the literature. The diffusivity of water is lower in the binary mixture than in the pure water system. Chen and co-workers [27] also reported the low value of water diffusion in glycerol compared to a pure water system. The decrease of individual molecule diffusivity in a binary mixture compared to a pure system is primarily due to the resistance from Fick's law and the formation of hydrogen bonding between the molecules [28]. The diffusion coefficient of mefenamic acid in mefenamic acid/water, which is 2.444×10^{-10} m^2 s^{-1}, on the other hand, is much lower than the normal diffusion coefficient value in a liquid solution. The

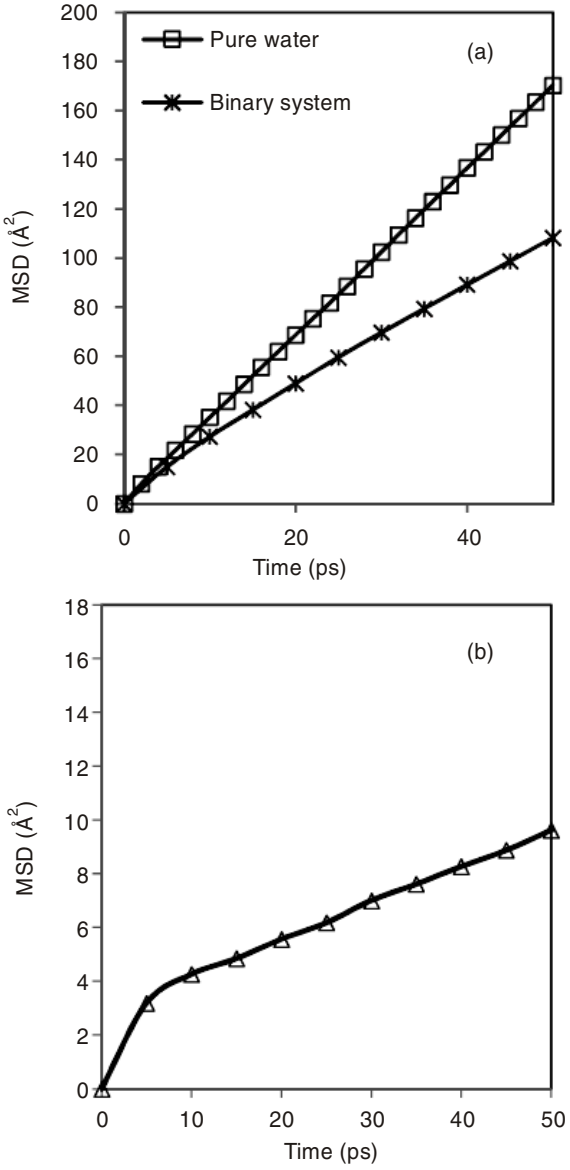

Fig. 3. (a) Mean squared displacement of water in a pure system in comparison with in the binary system of mefenamic acid/water; (b) Mean squared displacement of mefenamic acid in the mefenamic acid/water system

TABLE-2
DEVIATION OF AVERAGE SIMULATED DENSITIES AND TEMPERATURES FROM PRESENT MOLECULAR DYNAMICS SIMULATIONS WHEN SETTING PARAMETERS AT 0.1 MPa

System	Average Density (g/cm^3)		Deviation (%)[b]	Temperature (K)		Deviation (%)[b]
	Simulated value	Setting value		Simulated value	Setting value	
Pure water	0.964	0.997 [19]	3.31	306.02	298	2.68
Mefenamic acid/Water	1.068	1.136	5.99	296.54	298	0.49

[b]Deviation = [(Simulated value – Calculated value) / Calculated value] × 100

low value of mefenamic acid diffusivity in water indicates that the mefenamic acid is difficult to diffuse or soluble through water molecules. This behaviour would reflect the mefenamic acid character that tends to form a phase separation and do not dissolve in water as illustrated in Fig. 4(b). As seen in Fig. 4(a), the mefenamic acid molecules were randomly scattered at the beginning of the simulation before force field was applied to the simulation system. When simulation were run up to 2 ns, a phase separation was observed between mefenamic acid and water in the final trajectory frame as illustrated in Fig. 4(b).

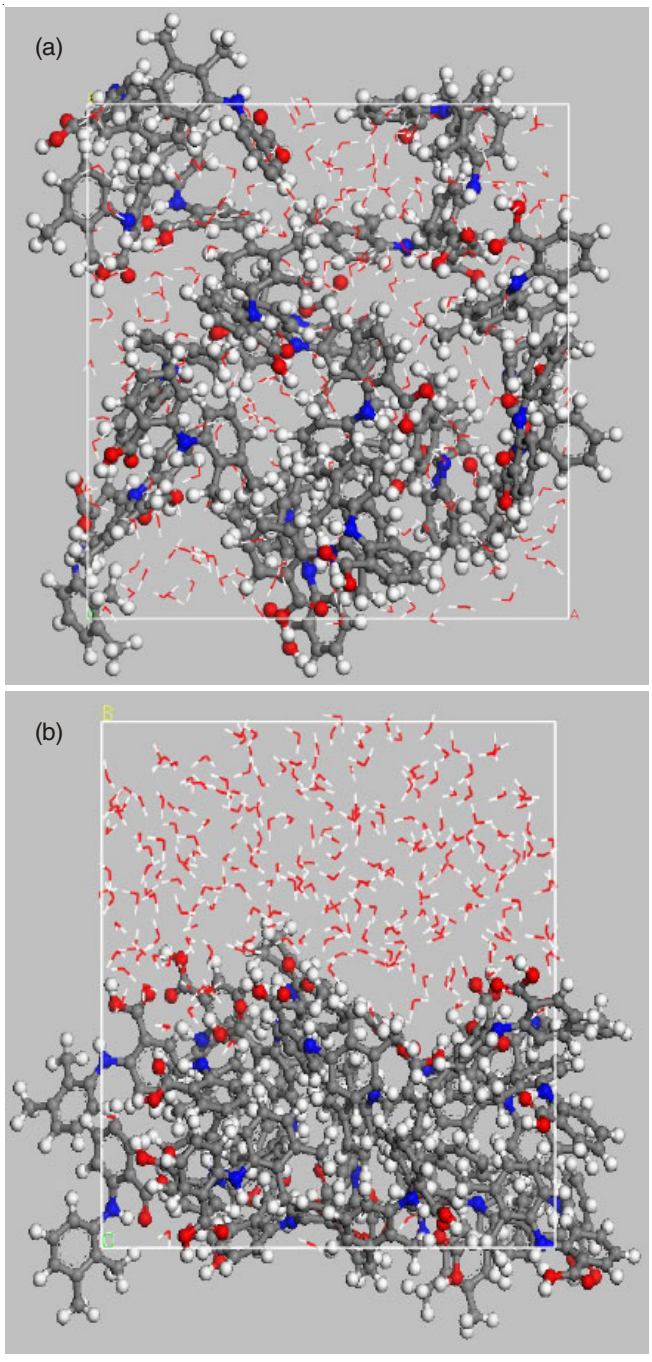

Fig. 4. Simulation box viewed from the xy-plane showing: (a) the initial distribution of mefenamic molecules in water; (b) the final distribution of mefenamic acid molecules in water. The mefenamic acid molecules are shown in the ball and stick style, while the water molecules are in the line style

Intermolecular Interactions in binary system: During dissolution process, the distribution of solute molecules within the solvent will occur. This process involves the attraction and association of molecules of a solvent with the molecules of the solute. Solute molecules that are soluble in the targeted solvents will normally take positions that are initially taken by the solvent molecules. Solute molecules will dissolve in a solvent when it forms favourable interactions with the solvent [29]. Fig. 5 illustrates the van't Hoff plot of mefenamic acid solubility in water which was constructed based on the solubility data reported in the literature [8]. The ideal solubility data illustrated was calculated using the ideal van't Hoff equation as below:

$$\ln x = \frac{\Delta H_f}{R}\left(\frac{1}{T_f} - \frac{1}{T}\right) \quad (3)$$

where x is the mole fraction of the solute in the solution, ΔH_f is the molar enthalpy of fusion of the solute (J/mol), R is the gas constant, T_f is the fusion temperature of the solute (K) and T is the solution temperature (K). The value of the molar enthalpy of fusion and the fusion temperature are 36.86 kJ mol^{-1} and 504.65 K, respectively [30]. As seen in Fig. 5, the solubility line of mefenamic acid in water, is below than the ideal solubility line. This indicates poor interaction between the mefenamic acid (solute) and water (solvent) molecules in comparison with the solvent-solvent and solute-solute interaction. This is because, the van't Hoff plot of the solute/solvent system that show similar interactions shall approach the ideal solubility line. Meanwhile, the solubility line of binary system that show good solute-solvent interaction shall located above the ideal solubility line.

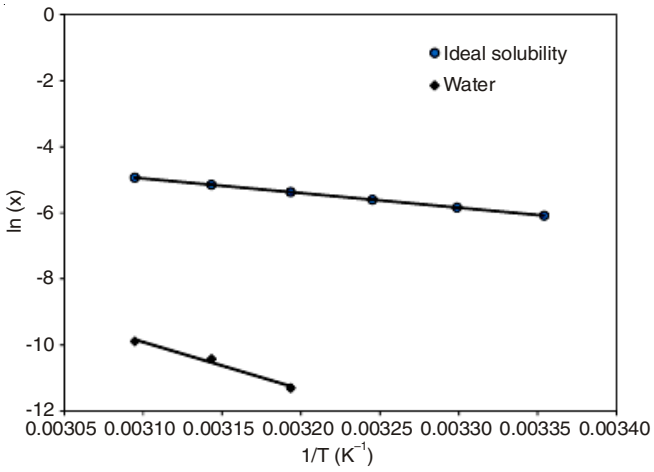

Fig. 5. van't Hoff plot of mefenamic acid solubility and ideal solubility values

In addition to van't Hoff plot, the molecular behaviour during the dissolution process that depends on the relative forces of the intermolecular interactions, namely solvent-solvent, solute-solvent and solute-solute can be described using radial distribution function [29]. Fig. 6 shows a significant change in the radial distribution function intensities for pure water (O1W···H1W) after the addition of mefenamic acid into the system. The changes is in line with the differences in the self-assembly of solvent-solvent molecules that are present

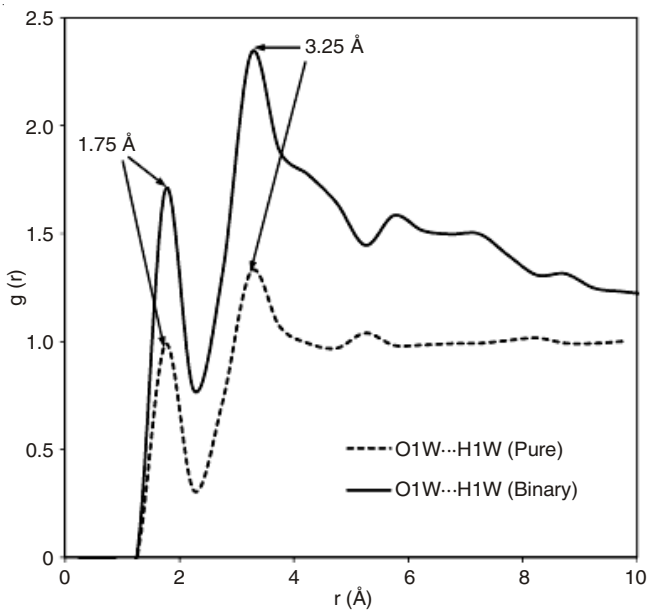

Fig. 6. Comparison of radial distribution functions between water molecules, O1W···H1W, in binary and pure systems to represent the solvent-solvent interactions

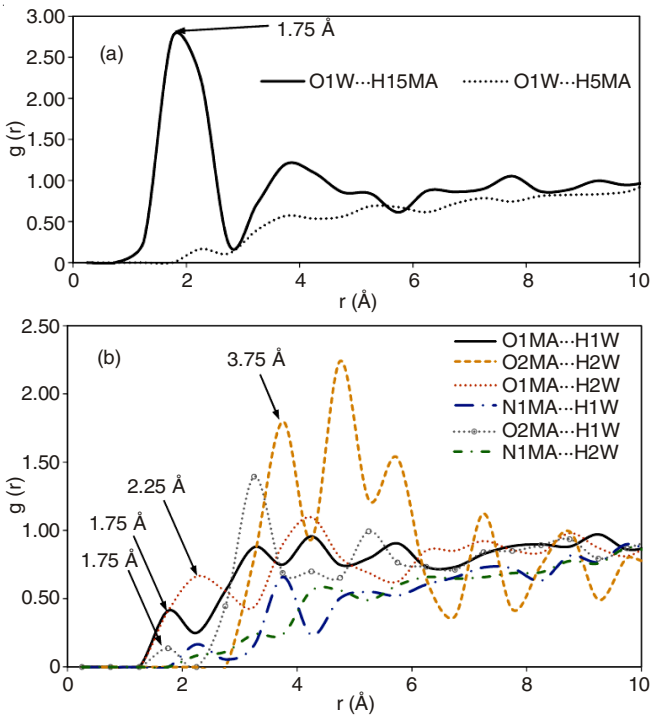

Fig. 7. Radial distribution functions between atoms in mefenamic acid molecules and in water molecules to represent the solute-solvent interactions

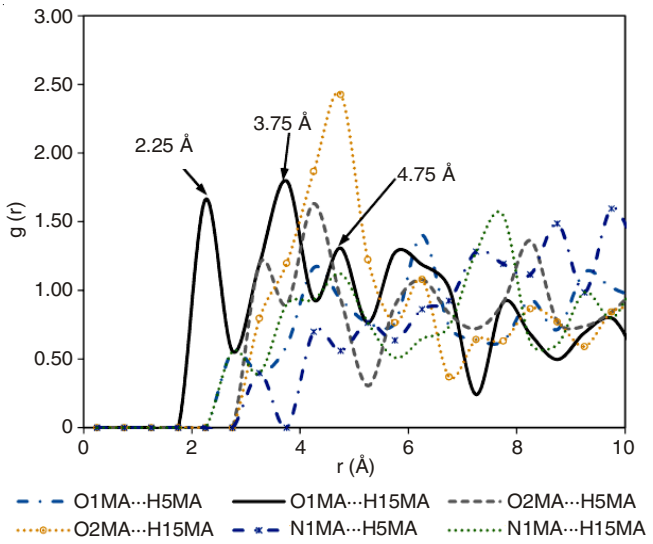

Fig. 8. Interactions between molecules of mefenamic acid in the mefenamic acid/water system to represent the solute-solute interactions

in the binary solution, but not present in the pure solvent. The presence of two strong peaks at 1.75 and 3.25 Å with higher intensities confirms the strong hydrogen bonding interaction between the water molecules.

The probabilities of solvent-solute interactions in the mefenamic acid/water system are shown in Fig. 7. The radial distribution function of O1W···H5MA, NIMA···H1W and N1MA···H2W are less structured with no sharp peak and do not follow the general simple liquid radial distribution function structure [31,32]. Other radial distribution functions which are O1W···H15MA, O1MA···H1W, O1MA···H2W, O2MA···H1W, and O2MA···H2W are less structured with the first peak shown at radial distance of 1.75, 1.75, 2.25, 1.75 and 3.75 Å, respectively. The radial distribution function of O1W···H15MA is the strongest as it shows the highest probability value which is 2.75 at a radial distance of 1.75 Å. These findings may suggest that the hydrogen bonds formed by O1W···H15MA plays a significant role in the association of mefenamic acid molecules in water.

The probabilities of intermolecular interactions between the mefenamic acid molecules are illustrated in Fig. 8. The strength of these interactions depends on the radius distance of the mefenamic acid molecules from the mefenamic acid reference molecule. As seen in Fig. 8, the g (r) of O1MA···H15MA shows the sharpest peak with an intensity of 1.65 at the nearest radial distance which is 2.25 Å. Thus, it can be suggested to represent the solute-solute interaction in the binary mixture of mefenamic acid/water. This solute-solute interaction, however, follow the general radial distribution function pattern of a solid system [31] as it shows several intense peaks at a radial distance of 2.25, 3.75 and 4.25 Å. The radial distribution functions pattern between mefenamic acid molecules that follow the radial distribution function pattern of the solid system may suggest that the mefenamic acid molecules in the mixture remain in solid form. This finding explains the phase separation that exists between mefenamic acid and water molecules (Fig. 7b) as well as the poor solubility behaviour of mefenamic acid in water at low temperature as reported in the literature [8].

Conclusion

In this work, molecular dynamics simulations (MD) have been performed for pure water molecules and the binary system of mefenamic acid/water. The simulated radial distribution function patterns and diffusivities for pure water using the COMPASS force field and the Ewald summation method show good agreement with simulations in the literature. The small deviation between simulated densities and the setting value suggest the validity of simulation method employed. The simulation for the binary mixture of mefenamic acid/water shows

that strong hydrogen bonding was formed between water molecules. However, less intense intermolecular interactions were established between mefenamic acid molecules and water. These findings are in agreement with the van't Hoff plot of the mefenamic acid solubility in water which is lower than the ideal solubility line. The nature of these interactions explains the low diffusivity and poor solubility values of mefenamic acid in water.

ACKNOWLEDGEMENTS

One of the authors (SKAM) is grateful to the Malaysian Ministry of Higher Education and University Malaysia Pahang for a scholarship. The work was financially supported by the International Islamic University Malaysia (Research Acculturation Grant Scheme RAGS 12-026-0026) and the University Malaysia Pahang (Exploratory Research Grant Scheme RDU120607).

REFERENCES

1. S. Güngör, A. Yildiz, Y. Özsoy, E. Cevher and A. Araman, *IL Farmaco*, **58**, 397 (2003).
2. D.N. Bateman, *Medicine*, **40**, 140 (2012).
3. L. Fábián, N. Hamill, K.S. Eccles, H.A. Moynihan, A.R. Maguire, L. McCausland and S.E. Lawrence, *Cryst. Growth Des.*, **11**, 3522 (2011).
4. S. Cesur and S. Gokbel, *Cryst. Res. Technol.*, **43**, 720 (2008).
5. R. Panchagnula, R. Sundaramurthy, O. Pillai, S. Agrawal and Y.A. Raj, *J. Pharm. Sci.*, **93**, 1019 (2004).
6. S.B. Pedersen, *Pharmacol. Toxicol.*, **75**, 22 (1994).
7. J.W. Mullin, Crystallization, Butterworth-Heinemann, Oxford, edn 4, (2001).
8. S.K. Abdul Mudalip, M.R. Abu Bakar, P. Jamal and F. Adam, *J. Chem. Eng. Data*, **58**, 3447 (2013).
9. J. Wang and D.R. Flanagan, Fundamentals of Dissolution, Elsevier, Burlington, MA (2009).
10. D.C. Sperry, S.J. Thomas and E. Lobo, *Mol. Pharm.*, **7**, 1450 (2010).
11. Y. Gao and K.W. Olsen, *Mol. Pharm.*, **10**, 905 (2013).
12. D. Toroz, R. Hammond, K. Roberts, S. Harris and T. Ridley, *J. Cryst. Growth*, **401**, 38 (2014).
13. P.R. Burkholder, G.H. Purser and R.S. Cole, *J. Chem. Educ.*, **85**, 1071 (2008).
14. S.K.A. Mudalip, M.R.A. Bakar, F. Adam and P. Jamal, *Int. J. Chem. Eng. Appl.*, **4**, 124 (2013).
15. Q. Yi, J. Chen, Y. Le, J. Wang, C. Xue and H. Zhao, *J. Cryst. Growth*, **372**, 193 (2013).
16. J. Gupta, C. Nunes, S. Vyas and S. Jonnalagadda, *J. Phys. Chem. B*, **115**, 2014 (2011).
17. H. Abdel-Halim, D. Traini, D. Hibbs, S. Gaisford and P. Young, *Eur. J. Pharm. Biopharm.*, **78**, 83 (2011).
18. H. Sun, *J. Phys. Chem. B*, **102**, 7338 (1998).
19. N. Calvar, E. Gómez, B. González and Á. Domínguez, *J. Chem. Thermodyn.*, **41**, 939 (2009).
20. A.O. Surov, I.V. Terekhova, A. Bauer-Brandl and G.L. Perlovich, *Cryst. Growth Des.*, **9**, 3265 (2009).
21. M.P. Allen and D.J. Tildesey, Computer Simulation of Liquids, Oxford University Press, New York (1991).
22. A.S. Nose, *J. Chem. Phys.*, **81**, 511 (1984).
23. H.J.C. Berendsen, J.P.M. Postma, W.F. van Gunsteren, A. Di Nola and J.R. Haak, *J. Chem. Phys.*, **81**, 3684 (1984).
24. S. Hamad, C. Moon, C.R.A. Catlow, A.T. Hulme and S.L. Price, *J. Phys. Chem. B*, **110**, 3323 (2006).
25. F. Adam, Ph.D. Thesis, Institute of Particle Technology, University of Leeds, Leeds (2012).
26. P. Mark and L. Nilson, *J. Phys. Chem. A*, **105**, 9954 (2001).
27. C. Chen, W.Z. Li, Y.C. Song, L.D. Weng and N. Zhang, *Mol. Phys.*, **110**, 283 (2012).
28. C. Dimitroulis, E. Kainourgiakis, V. Raptis and J. Samios, *J. Mol. Liq.*, **205**, 46 (2015).
29. B. Lindman, G. Karlström and L. Stigsson, *J. Mol. Liq.*, **156**, 76 (2010).
30. S. Romero, B. Escalera and P. Bustamante, *Int. J. Pharm.*, **178**, 193 (1999).
31. A.R. Leach, Molecular Modelling: Principles and Applications, Prentice Hall, England (2001).
32. T.S. Ingebrigtsen, T.B. Schroder and J.C. Dyre, *Phys. Rev. X*, **2**, 011011 (2012).